Biochimica et Biophysica Acta 1859 (2017) 40–47

Contents lists available at ScienceDirect

Biochimica et Biophysica Acta

journal homepage: www.elsevier.com/locate/bbamem

Disentangling protein and lipid interactions that control a molecular switch in photosynthetic light harvesting

Emanuela Crisafi, Anjali Pandit *

Leiden Institute of Chemistry, Dept. of Solid-State NMR, Leiden University, Einsteinweg 55, 2333CC Leiden, The Netherlands

ARTICLE INFO

Article history:
Received 11 June 2016
Received in revised form 30 September 2016
Accepted 21 October 2016
Available online 26 October 2016

Keywords:
LHCII
Non-photochemical quenching
Lipid nanodiscs
Membrane reconstitution
Fluorescence spectroscopy
Circular dichroism

ABSTRACT

In the photosynthetic apparatus of plants and algae, the major Light-Harvesting Complexes (LHCII) collect excitations and funnel these to the photosynthetic reaction center where charge separation takes place. In excess light conditions, remodeling of the photosynthetic membrane and protein conformational changes produces a photoprotective state in which excitations are rapidly quenched to avoid photodamage. The quenched states are associated with protein aggregation, however the LHCII complexes are also proposed to have an intrinsic capacity to shift between light harvesting and fluorescence-quenched conformational states. To disentangle the effects of protein-protein and protein-lipid interactions on the LHCII photoprotective switch, we compared the structural and fluorescent properties of LHCII lipid nanodiscs and proteoliposomes with very low protein -to-lipid ratios. We demonstrate that LHCII proteins adapta fully fluorescent state in nanodiscs and in proteoliposomes with highly diluted protein densities. Increasing the protein density induces a transition into a mildly-quenched state that reaches a plateau at a molar protein-to-lipid ratio of 0.001 and has a fluorescence yield reminiscent of the light-harvesting state *in vivo*. The low onset for quenching strongly suggests that LHCII-LHCII attractive interactions occur inside membranes. The transition at low protein densities does not involve strong changes in the excitonic circular-dichroism spectrum and is distinct from a transition occurring at very high protein densities that comprises strong fluorescence quenching and circular-dichroism spectral changes involving chlorophyll 611 and 612, correlating with proposed quencher sites of the photoprotective mechanisms.

1. Introduction

Photosynthetic light-harvesting antennae form supra-molecular arrays with strong connectivity that capture sunlight and transfer the excitations over long distances towards the photosynthetic reaction centers, where charge separation takes place. In contrast to artificial solar antennae, natural light-harvesting structures are dynamic assemblies that continuously adapt to the light conditions for prevention of photo damage. In excess light, extensive remodeling of the photosynthetic thylakoid membranes takes place. The ability of the peripheral light-harvesting complexes (LHCII) of plants and photosynthetic algae to adapt fluorescent, light harvesting, versus photoprotective, excitation-quenched states under excess light conditions, is a phenomenon that has been studied extensively *in vivo* and *in vitro* over the last decade [1–7]. LHCII proteins have the intrinsic capacity to switch between light harvesting, fluorescent, or photo protective, quenched conformational states [2,8]. The formation of excitation-quenched states is associated with LHCII aggregation in the membrane and the balance between light harvesting and photo protection is regulated by membrane remodeling under high light conditions [6,9]. Mild dilution with thylakoid lipids of overcrowded mutant thylakoid membranes has shown to increase the LHCII chlorophyll (Chl) fluorescence lifetimes, while further dilution uncouples the LHCII antenna proteins from the photosystem reaction-center units, breaking the connectivity [10,11]. Thus, the functional roles of the light-harvesting proteins to (1) transfer excitations to the photosynthetic reaction centers or (2) dissipate excess excitations under high light critically depend on the respective protein to lipid densities within strong- or weak-coupling regimes. The strong correlation between quenching and protein aggregation *in vivo* and *in vitro* together with the notice that individual LHCII complexes can adapt different fluorescent states, suggests a mechanistic process in which external pressure and protein or lipid changes in the LHCII microenvironment bring about a molecular conformational change. This change must involve altered chlorophyll (Chl)-xanthophyll or Chl-Chl interactions to quench the light excitations. While several models have been proposed for the photophysical quenching mechanisms [3,12–14] involving the protein-bound Chls, lutein and/or zeaxanthin, there is no clear view on the mechanistic process or on the protein conformational switch that is associated with a twist in

Abbreviations: β-DM, n-Dodecyl β-D-maltoside; CD, circular dichroism; Chl, chlorophyll; DGDG, digalactosyldiacylglycerol; DLS, dynamic light scattering; EM, electron miscroscopy; LHCII, light harvesting complex II; Lut, lutein; MGDG, monogalactosyldiacylglycerol; MSP, MSP1E3D1 membrane scaffold protein; Neo, neoxanthin; PG, phosphatidylglycerol; PLR, protein to lipid ratio, defined as mol LHCII trimer per moles of lipids; PSII, photosystem II; SQDG, sulfoquinovosyldiacylglycerol; T, transmission.

* Corresponding author.
E-mail address: a.pandit@chem.leidenuniv.nl (A. Pandit).

http://dx.doi.org/10.1016/j.bbamem.2016.10.010
0005-2736/

the protein-bound neoxanthin (Neo),a change in Chl *b* hydrogen bond strength [13], subtle changes in the Chl *a*ground-state electronic structures [15,16] and conformational changes in one of the luteins (Lut1) [17]. Upcoming methods, like single-molecule fluorescence and nuclear magnetic resonance (NMR) are being explored to comprehend the conformational switch of LHCII and its associated mechanistic process [2, 15]. The relevance of such studies strongly relies on the chosen *in-vitro* conditions to mimic the *in-vivo* membrane environment. In addition, recently new kinetic models have been proposed to describe excitation diffusion and quenching in small LHCII aggregates [18,19],which benefit from experimental data describing the behavior of single and aggregated LHCII under controlled, membrane-mimicking conditions.

Model lipid membranes form suitable tools for investigation of protein structure, dynamics and lipid interplay in a controlled environment and open possibility to create artificial minimal protein networks with functional connectivity. LHCII-reconstituted proteoliposomes and protein-lipid aggregates have been investigated to determine inter-protein connectivity and protein-lipid interactions under various conditions [20–22]. Comparing the structural and functional properties of aggregated membrane proteins in proteoliposomes with those of isolated proteins embedded in detergent micelles, however, creates a bias because the protein microenvironment changes when proteins are transferred from detergent micelles to lipid membranes. Lipid nanodiscs form attractive alternative model systems that prevent protein aggregation, but provide a lipid environment. We demonstrated that LHCII proteins could be reconstituted in asolectin lipid nanodiscs, capturing the proteins in their fluorescent, light-harvesting state [23].

In this work we compared the structure and fluorescence properties of LHCII in lipid nanodiscs with LHCII proteoliposomes, disentangling protein-protein and protein-lipid interactions in minimal membrane models to investigate the LHCII mechanistic, functional switch. The LHCII pigment-protein complexes are unique in possessing chlorophylls (Chls) and xanthophylls that form intrinsic probes, reporting changes in the microenvironment. By adjusting the protein to lipid ratio in the proteoliposomes, we determined the onset ratio for protein aggregation in membranes, bridging the gap between properties of isolated proteins and of their aggregated states. Liposome and nanodisc models were prepared from plant thylakoid or from soybean asolectin lipids to investigate the influence of specific lipid microenvironments. Thylakoid lipids were used to mimic the lipid composition of native thylakoid membranes. Preparations of soybean asolectin lipids were used as easy-controllable lipid model systems and for comparison of our data with previous results obtained in an earlier study on LHCII lipid nanodiscs [23]. Circular dichroism (CD) experiments were carried out to characterize LHCII pigment interactions inside the different membrane models.

2. Materials and methods

2.1. LHCII extraction

Light harvesting complexes were purified from spinach leaves (*Spinacea aloracea*) as described previously [23]. In short, LHCII trimer complexes were isolated using a sucrose gradient. The green band of LHCII trimmers was manually collected with a long needle. The purified LHCII complexes were characterized by absorption spectroscopy, buffer-exchanged into buffer containing 50 mM HEPES, 100 mM NaCl, pH = 7.5, 0.03% *n*-Dodecyl β-D-maltoside (β-DM, purchased from Sigma) and concentrated using Amicon Ultra 2 ml centrifugal filters with cut off of 30 K (Millipore). The protein complexes were stored at −80 °C until use.

2.2. Preparation of asolectin liposomes

Chloroform was added to asolectin from soybean lipids (purchased from Sigma) to a concentration of 5 mg/ml. The chloroform/asolectin solution was collected in a round-bottom flask, and all solvent was evaporated with a stream of N_2 followed by evaporation in a rotary evaporator (R3000, Buchi). The phospholipid bilayer was then hydrated using the reverse phase method. A solution was poured to the dried film containing buffer (50 mM HEPES, 100 mM NaCl, pH = 7.5) and diethyl ether in the ratio 1 to 3, and gently mixed and sonicated (2210 Branson). The diethyl ether was evaporated using the rotary evaporator and the last traces of solvent were removed using a stream of N_2. The liposome suspensions were exposed to 10 freeze/thaw cycles followed by extrusion through polycarbonate membranes of 400 and 200 nm pore size, using a mini extruder (Avanti polar lipids, Alabama). Sizes of liposome preparations were determined by dynamic light scattering (DLS) using a Malvern Zetasizer Nano ZS equipped with a Peltier-controlled thermostatic cell holder.

2.3. Preparation of thylakoid-lipid liposomes

Thylakoid lipids phosphatidylglycerol (PG), digalactosyldiacylglycerol (DGDG), monogalactosyldiacylglycerol (MGDG) and sulphoquinovosyl diacylglycerol (SQDG) were purchased from Lipid Products Company (Redhill, UK). Unilamellar liposomes were prepared according to [24]. Lipid mixtures containing 47% MGDG, 27% DGDG, 12% SQDG and 14% PG were dried into a thin film using a rotary evaporator at 40 °C, to remove all traces of chloroform. The lipid film was hydrated using reconstitution buffer (50 mM HEPES, 100 mM NaCl, pH = 7.5 and0.03% β-DM) to a final lipid concentration of 0.25 mg/ml. Detergent was extracted by 48-hrs incubation with polystyrene beads (Biobeads, SM-2, Bio Rad). The liposome suspensions were exposed to 10 freeze-thaw cycles followed by extrusion through polycarbonate membranes with 200 nm and 100 nm pore sizes.

2.4. Protein insertion in liposomes

To determine the onset of liposome solubilization by detergent, liposome preparations were titrated with β-DM and DLS was used to monitor the solubilization of liposomes into lipid-detergent micelles as described in the Supplementary Information (SI) section (Figs. S1 and S2). The onset value for solubilization was determined as 0.01% β-DM for liposome preparations containing 0.95 mM lipid, which converts to 5 lipids per detergent molecule. Because the LHCII preparations required 0.03% β-DM at least for their solubilization, we especially checked effect of liposome destabilization with 0.02–0.04% β-DM. At these detergent concentrations, the majority of the liposomes were still intact according to the light-scattering profiles.

For protein insertion, preformed liposomes were destabilized by addition of 0.03% of β-DM to facilitate insertion of LHCII into the liposome membranes. LHCII complexes were added to the liposome suspension and incubated for 30 min. For proteoliposome preparations with very high protein to lipid ratios (1:65), instead of insertion into preformed liposomes, the LHCII complexes in β-DM were mixed with detergent-solubilized lipids to ensure proper mixing of the lipids and LHCII proteins. Bio beads were added to the suspensions in several steps and solutions were incubated overnight. The proteoliposome suspensions were centrifuged at 15,000*g* for 30 min at 4 °C using a table-centrifuge 5430 R (Eppendorf, Germany) to remove non-incorporated LHCII that forms aggregate pellets. A sucrose gradient analysis confirmed the absence of non-incorporated LHCII (SI section, Fig. S4). The proteoliposome preparations were structurally characterized by cryo-electron microscopy (cryo-EM) performed on a FEI Technai T20 electron microscope, operating at 200 keV.The reported protein to lipid ratios (PLR) are defined as moles of LHCII trimers per moles of total lipids. The concentration of LHCII trimers was determined from the molair extinction coefficient for LHCII (trimers) at 670 nm, $\varepsilon = 1{,}638{,}000\ M^{-1}\ cm^{-1}$ [25].

2.5. Preparation of LHCII asolectin nanodiscs

For incorporation of LHCII in lipid nanodiscs, we used the membrane scaffold protein (MSP) MSP1E3D1 [26]. MSPs are amphiphatic helices and are genetically engineered proteins, which mimic the function of Apolipoprotein A-1. Lipid nanodiscs are formed spontaneously upon detergent extraction of lipid/detergent/MSP mixtures. In lipid nanodiscs, the lipid molecules associate as a bilayer domain while two molecules of MSP wrap around the edges of the discoidal structure in a belt-like configuration, one MSP covering the hydrophobic alkyl chains of each leaflet. For preparation of LHCII asolectin nanodiscs, a solution 5 mg/ml of asolectin was prepared according to [23] in buffer (50 mM HEPES, 100 mM NaCl, pH = 7.5) with 40 mM nonyl β-D-glucopyranoside (Sigma-Aldrich). The formed solutions were clear without suspension. LHCII complexes were mixed with the lipid/detergent solutions and incubated at 4 °C shaking for 15 min. The membrane scaffold protein MSP1E3D1 (overexpressed from *E. coli* according to [23]) was added to the mixture and incubated for another 15 min. To allow the reconstitution of protein in nanodiscs, the detergent was removed using Bio-beads SM-2. Samples were diluted to a final volume of 2 ml and ultra-centrifuged at 37,000 rpm (120,000 *g*) at 4 °C to remove lipid and protein pellets, in an Optima L-90K Ultracentrifuge (Beckman Coulter)using a 70.1 Ti rotor. Because we observed that for some preparations small aggregates remained in the lower part of the supernatant, the upper and lower milliliter volumes of the 2 ml supernatant solution were collected separately from the centrifuge tubes. Sizes of empty nanodisc and liposome preparations were determined by DLS. The illumination wavelength of the DLS apparatus, 632.8 nm, was not suitable for measuring scattering profiles of LHCII-containing samples that scattered fluorescence upon illumination, disturbing the dynamic light-scattering profiles.

2.6. Preparation of LHCII thylakoid-lipid nanodiscs

Nanodiscs consisting of plant thylakoid lipids were prepared as described above for asolectin lipid nanodiscs, except for the initial step. Lipid mixtures containing 47% MGDG, 27% DGDG, 12% SQDG and 14% PGor lacking MGDG, containing 61.9% DGDG, 16.7% SQDG and 21.4% PG were dried with a rotary evaporator for 45 min at 40 °C. The lipid film was hydrated with buffer (50 mM HEPES, 100 mM NaCl, pH = 7.5) containing 40 mM nonyl β-D-glucopyranoside. The remaining steps were performed following the protocol described above for asolectin lipids.

2.7. CD measurements

CD spectra were recorded on a J-815 spectrometer (Jasco, Gross-Umstadt, Germany) equipped with a temperature control set. The wavelength range was from 350 to 750 nm, data pitch 1 nm, response 2 s, band width 4 nm and scanning speed 50 nm/min at 20 °C using 0,2 or 0,5 cm quartz cuvette (Hellma, Germany).

2.8. UV/VIS measurements

Absorption spectra were recorded on a UV-1700 PharmaSpec UV–visible spectrophotometer (Shimadzu, Japan) with the wavelength range was set from 350 to 750 nm.

2.9. Fluorescence measurements

Fluorescence measurements were performed on a Cary Eclipse fluorescence spectrophotometer (Varian), collecting emission spectra from 660 to 720 nm using 3 mm quartz cuvettes. The optical density of the sample preparations varied from 0.03 to 0.07 cm^{-1} at 650 nm The excitation wavelength was set at 650 nm or 475 nm. Fluorescence quantum yields of LHCII proteoliposome and nanodisc preparations were determined relative to the fluorescence yield of LHCII in β-DM, corrected for the number of absorbed photons by dividing fluorescence intensities by 1-T (T = transmission). To minimize errors caused by liposome scattering, which causes a scattering background signal at the blue side of the absorption spectra (see SI section, Fig. S3), liposome samples were excited at the red side in the Q_y band of Chl *b* (λ_{exc} = 650 nm) and fluorescence emission spectra were corrected for the number of absorbed photons by dividing the fluorescence intensities by $1\text{-}T_{650}$.

3. Results and discussion

3.1. Fluorescence analysis of LHCII in nanodiscs composed of asolectin or thylakoid lipids

LHCII lipid nanodiscs were prepared using soybean asolectin lipids, according to Pandit et al. [23], or using a mixture of plant thylakoid lipids as mentioned in the Materials and methods section. Native thylakoid membranes contain the non-bilayer lipid MGDG that makes up ~40–50% of the lipid constituents [27]. The addition of MGDG however to our lipid preparations prevented the formation of nanodiscs and resulted in the formation of LHCII lipid aggregates. MGDG is a non-bilayer lipid that changes the membrane lateral pressure profile and has a preference for hexagonal membrane phases [28]. The cone-shaped MGDG lipids might prevent the formation of flat lipid membrane discs that are stabilized by the MSP proteins. At optimized LHCII:MSP:lipid ratios, both the asolectin and DGDG/SQDG/PG LHCII-lipid nanodiscs had fluorescence intensities that were90–100% compared to the fluorescence intensities of LHCII in β-DM micelles (Table S1, SI section), while in sub-optimal LHCII:MSP:lipid ratios lower fluorescence yields are observed, caused by small amounts of LHCII aggregates that quench the fluorescence (see also [23]). The asolectin lipid LHCII nanodisc preparations required protein to lipid ratios (PLRs) up to1:120, which for LHCII is equivalent to a Chl to lipid ratio of 1:3. Note that in lipid membranes where the LHCII proteins would not be prevented from protein-protein interactions by the MSPs, such high PLR would correspond to highly aggregation-induced quenched states of LHCII [29],confirming that the nanodisc scaffolds prevent LHCII aggregation. In earlier work, we already demonstrated that LHCII retains its fluorescent state upon reconstitution in asolectin nanodiscs [23]. Here we conclude that LHCII also adapts an unquenched, fully fluorescent state in nanodiscs composed of thylakoid lipids.

3.2. Fluorescence analysis of LHCII proteoliposomes at low protein to lipid ratios

In artificial and in native membranes, the fluorescence of LHCII is reduced compared to the fluorescence of LHCII in detergent micelles. The LHCII-nanodisc experiments suggest that fluorescence quenching is not caused by the transition from a detergent to a lipid environment, but is induced by LHCII aggregation. If this is the case, dilution of LHCII complexes in proteoliposome membranes should reproduce the fluorescence yields observed for the LHCII lipid nanodiscs. To test this assumption, we prepared LHCII asolectin proteoliposomes at very low PLR in the range $2 \cdot 10^{-5}$ (PLR = 1:50,000) to $2 \cdot 10^{-3}$ (PLR = 1:500). At the lowest ratios, the fluorescence yield indeed equals the fluorescence yields of LHCII in lipid nanodiscs or detergent micelles (Fig. 1). The fluorescence yield decreases rapidly with increased PLR until a plateau is reached where the yield is reduced to ~50% relative to the fluorescence of LHCII in lipid nanodiscs. A 50% yield relative to the fluorescence lifetime of LHCII in detergent micelles, for which lifetimes of 3.6 to 4 ns have been recorded [23], is comparable with the observed *in-vivo* LHCII averaged lifetimes under normal light conditions that are 1.0 to 2 ns [6,30]. Note that the fluorescence yield does not change over at least an order of magnitude between PLR = $2 \cdot 10^{-4}$ to

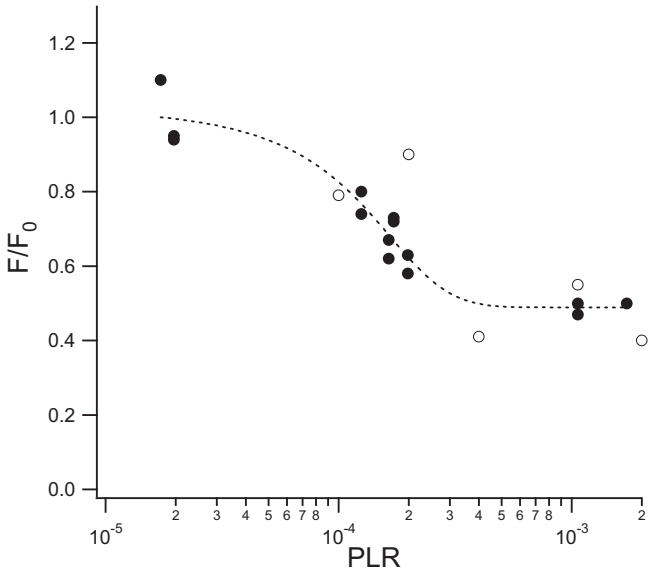

Fig. 1. Fluorescence yield (F) of LHCII asolectin proteoliposomes (black circles) and thylakoid MGDG/DGDG/SQDG/PG proteoliposomes (open circles) relative to the fluorescence of LHCII in β-DM micelles (F_0) at different protein to lipid ratios (PLR). To determine the midpoint PLR value, data of asolectin proteoliposomes was fit with a sigmoidal curve, with the following fit parameters: xhalve at PLR $= 1.0 \cdot 10^{-4} \pm 8.2 \cdot 10^{-5}$, maximal fluorescence reduction $= -0.67 \pm 0.31$ and Fmax $= 1.16 \pm 0.30$.

$2 \cdot 10^{-3}$, implying that quenching is not proportional to the protein densities in this range.

The asolectin LHCII proteoliposomes in our preparations had varying sizes according to different EM micrographs (Fig. 2). Assuming that (1) liposomes contain double-leaflet membranes in which each asolectin lipid molecule occupies a surface area of 70 Å^2 [31], (2) most of the liposomes have diameters in the 60–80 nm range (Fig. 2), and (3) discarding losses of LHCII or lipids during our preparations, we estimate that preparations with a PLR of $1 \cdot 10^{-4}$ (1:10,000, xhalve of the quenching curve in Fig. 1) contain 1 to 2 LHCII trimers *per vesicle*. The curve reaches a plateau value of ~50% quenching with on average 8–14 LHCII *per vesicle*, assuming vesicle sizes of 60–80 nm (Fig. 2). Although the calculations are a very rough estimate, the number simply that the onset for fluorescence quenching starts when only few LHCII complexes *per vesicle* are present, suggesting that the LHCII proteins have attractive interactions and form small aggregate clusters. Our previous study on LHCII-lipid nanodiscs showed that LHCII-lipid preparations containing disc particles with diameter sizes ranging from 12 to 50 nm, already display considerable quenching characteristics (fluorescence yields were reduced to 40% compared to LHCII in detergent micelles [23]). Hence, small clusters of LHCII are capable of significantly reducing the fluorescence. Interestingly, the estimated average number of LHCIIs per vesicle at which the fluorescence quenching reaches a plateau (8–14 trimers) approaches the experimentally determined range for functional domain sizes of LHCII *in vivo* (12–24 trimers, according to [32]).

LHCII proteoliposomes prepared from thylakoid MGDG/DGDG/SQDG/PG lipid mixtures displayed similar quenching characteristics. For these lipid mixtures however, it was more difficult to control the PLR without losses of protein and lipids, which were sometimes observed as small pellet after the centrifugation step, and only few PLR values are compared (open circles in Fig. 1). For consistency with the lipid compositions of the thylakoid lipid nanodiscs, we also prepared liposomes without MGDG. These preparations however, contained mixtures of lipid vesicles and planar lipid sheets (SI, fig. S3) in which the LHCII fluorescence was strongly quenched (yield 20% relative to LHCII in detergent micelles). The reduction of the fluorescence yield in these preparations is comparable to the reduction of fluorescence *in vivo* when photo protective states are formed [6,30].

Summarizing, the LHCII proteoliposome data confirm that LHCII fluorescence quenching is induced by LHCII-LHCII interactions and not by a (specific) lipid microenvironment.

The non-bilayer lipid MGDG has been suggested to play a role in controlling the photo protective states of LHCII. Here we show that LHCII reconstituted in thylakoid lipid membranes with MGDG (proteoliposomes) or without MGDG (nanodiscs) both adapts unquenched states as long as protein-protein interactions are minimized. Molecular interactions between LHCII and MGDG lipids apparently do not induce fluorescence quenching. The MGDG lipids clearly do have an effect on the mesoscale organization, disturbing the thermodynamic equilibrium that stabilizes the MSP-lipid nanodisc scaffolds and counteracting the formation of large two-dimensional flat lipid-bilayer sheets. In native, highly crowded, thylakoid membranes, LHCII aggregation is associated with reversible supramolecular membrane phase transitions [9]. In liposomes, MGDG and DGDG promote LHCII aggregation [20] and in LHCII-Photosystem II (*PSII*) liposomes, MGDG lipids increase the light-harvesting cross section, promoting LHCII-*PSII* interactions [21]. The different studies strongly suggest a functional role for MGDG in controlling the supramolecular interplay between light-harvesting proteins *in vivo*.

3.3. CD characterization of LHCII lipid nanodiscs and LHCII proteoliposomes

In LHCII pigment-protein complexes, excitonic Chl-Chl and carotenoid-Chl interactions give rise to pronounced exciton bands in the CD spectrum in visible region. The CD spectral shapes are very

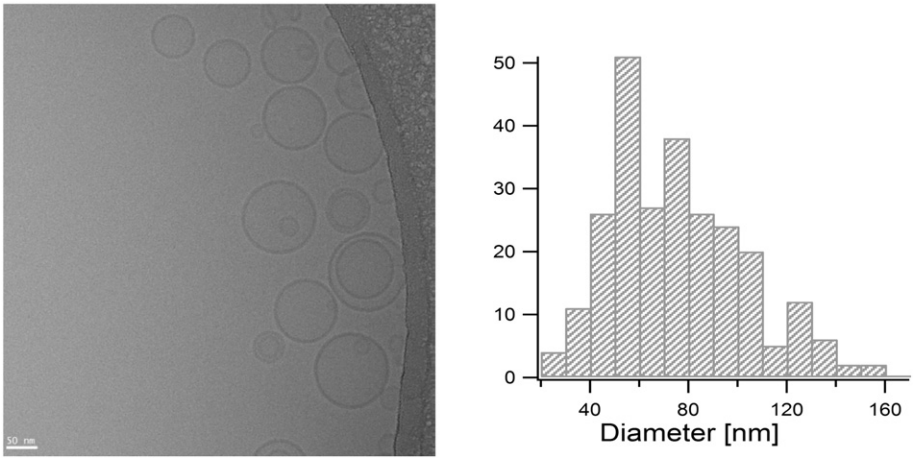

Fig. 2. Left: cryo-electron micrograph of asolectin LHCII proteoliposomes (scale bar 50 nm). Right: size distribution of asolectin liposomes, extracted from several electron micrographs.

sensitive to the LHCII pigment-protein folds and their microenvironment. To gain insight in the pigment-protein folds in different microenvironment and the influence of protein-lipid versus protein-protein interactions, we compared the exitonic CD spectra of LHCII in β-DM detergent micelles, lipid nanodiscs and proteoliposomes. Fig. 3 presents the CD spectra of LHCII in β-DM, LHCII in DGDG/SQDG/PG and asolectin nanodiscs and LHCII in MGDG/DGDG/SQDG/PG proteoliposomes with PLR = 1:555. In the Soret region, the negative peaks at (−)469 and (−)489 nm have similar intensities in the thylakoid lipid nanodiscs, while in proteoliposomes, the (−)469 band clearly has gained more strength relative to the 489 nm band. Increase in strength of the (−)469 nm band combined with a decrease of the (−)489 band has been attributed to stronger inter-monomer interactions within the LHCII trimers [33,34,]. The change in the 469/489 ratio observed for proteoliposomes suggests that LHCII-LHCII interactions in the membrane stabilize the trimers. The CD spectrum of asolectin nanodiscs also has a stronger −469 band than the spectrum of thylakoid lipid nanodiscs, suggesting that the environment of the asolectin lipids increases the stability of the LHCII trimers.

Fig. 4 shows CD difference spectra of LHCII thylakoid lipid nanodiscs minus LHCII in β-DM, and minus LHCII proteoliposomes. The changes in the 469/489 ratio associated with larger trimer stability in the proteoliposomes versus detergent micelles are reflected by the peak at 488 nm that is more prominent for the dashed spectrum (nanodiscs minus detergent). Remarkably, both difference spectra contain pronounced bands at (+)470 nm and (−)438 nm. The similar pattern of the two difference spectra suggests that the nanodisc *itself* influences the LHCII pigment microenvironments. Considering the size of the LHCII trimer complexes relative to the nanodisc dimensions (a triangular-shaped protein complex of ~6 nm wide embedded in a lipid disc of ~12 nm diameter), the surrounding MSP proteins could be in contact with the exterior xanthophyll and Chl pigments of LHCII. These pigments are the neoxanthin (Neo) that protrudes from the protein complexes, and the Chls *b*601, *b*605, *b*606, *b*608 and*a*610, *a*611, *a*612 and *a*614 (nomenclature according to Liu et al. [35]). Previous work demonstrated that changes occur in the Soret and Q_y band of absorption spectra of LHCII in lipid nanodiscs compared to detergent-solubilized LHCII, uncorrelated to fluorescence quenching [23]. These changes may also be explained by LHCII pigment interactions with the surrounding MSPs.

To compare proteoliposomes with low and high PLRs, thylakoid lipid proteoliposomes were prepared with three different PLRs of resp.1:2222, 1:555 and 1:65. The two lowest PLRs are in the regime

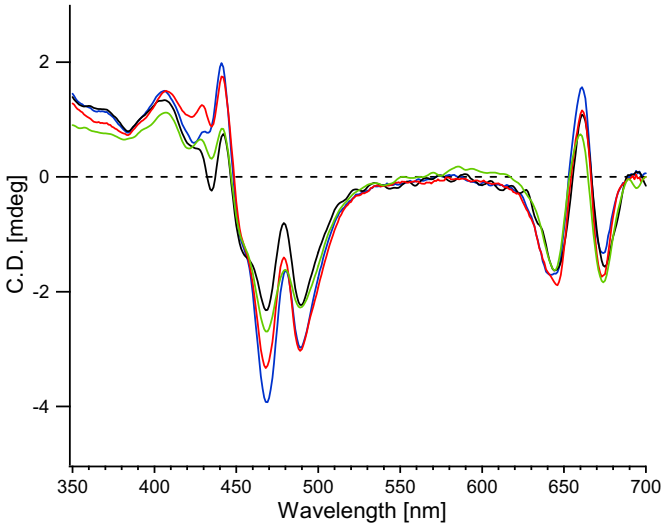

Fig. 3. C.D. spectra of LHCII in β-DM (*red*), LHCII in MGDG/DGDG/SQDG/PG proteoliposomes (PLR 1:555, *blue*), LHCII in DGDG/SQDG/PG nanodiscs (*black*) and LHCII in asolectin nanodiscs (*green*).

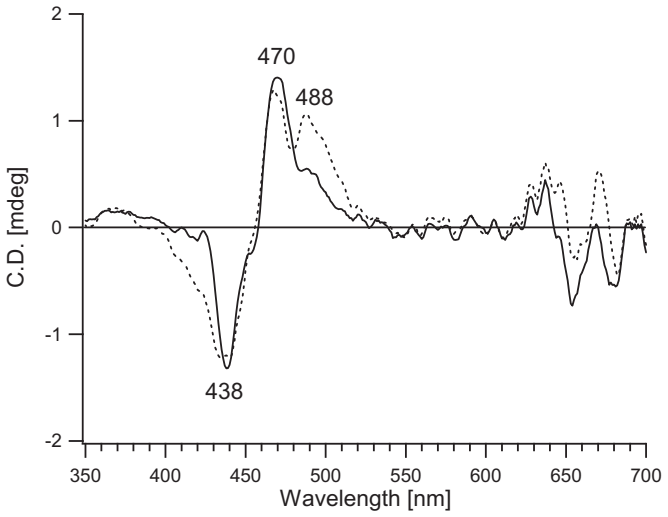

Fig. 4. C.D. difference spectrum of LHCII nanodiscs – LHCII β-DM (dashed) and LHCII nanodiscs – LHCII MGDG/DGDG/SQDG/PG proteoliposomes (solid line).

described in Fig. 1, where the fluorescence quenching is maximal ~50%, reminiscent of the light-harvesting states *in vivo* in the weak-coupling regime. Instead, the fluorescence of the densely packed proteoliposome preparations with PLR 1:65 was almost 10–15% quenched compared to LHCII in β-DM micelles (see Fig. 5). The quenching in these preparations is comparable with the fluorescence quenching in photo protective states *in vivo* [30]. Fig. 6 compares the CD spectra of LHCII proteoliposomes with different PLRs. The samples with PLRs of 1:2222 and 1:555 have quite similar excitonic CD spectra. As demonstrated in Fig. 1, changing the PLR in this regime also has only moderate effect on the fluorescence yields. For the highest PLR, specific spectral changes are observed that are indicated with the black arrows. The spectrum of proteoliposomes with PLR 1:65 resembles CD spectra of LHCII proteoliposomes reported in other work [34]. A comparison of this spectrum with the spectra of proteoliposomes with low PLRs allows us here to focus on the CD changes associated with the transition from a mild to strong fluorescence-quenched state.

Fig. 7 presents the CD difference spectrum of proteoliposomes with high PLR (1:65) minus low PLR (1:555). In the referred CD spectra in Fig. 6 we can exclude changes due to transitions from a detergent to a lipid environment. We presume that at a PLR of 1:555 the LHCII complexes are involved in weak protein-protein contacts, since the

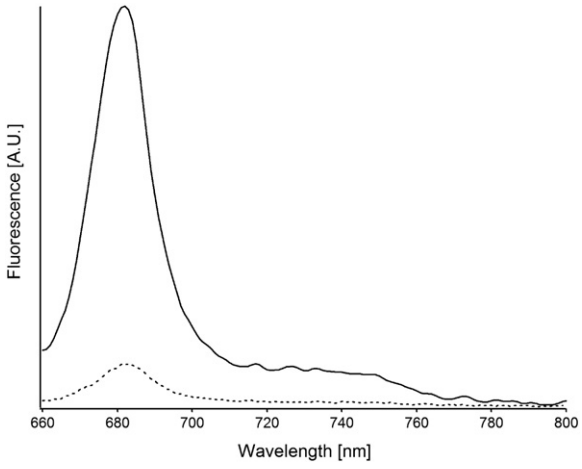

Fig. 5. Fluorescence emission of LHCII proteoliposomes with PLR = 1:65 (dotted line) compared to LHCII in *b*-DM (solid line) upon 650-nm excitation. Fluorescence intensities were scaled according to their relative transmission (T) at 650 nm, by dividing by the fluorescence intensities by (1-T).

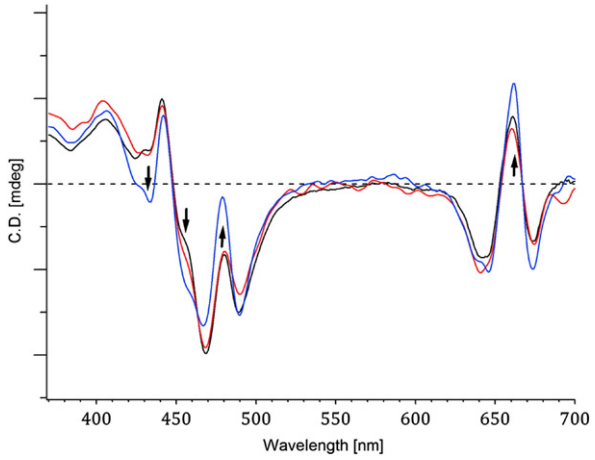

Fig. 6. CD spectra of LHCII in MGDG/DGDG/SQDG/PG proteoliposomes; PLR = (1:2222) in red, PLR = (1:555) in blue and PLR = (1:65) in black. Arrows indicate the most significant changes for PLR = 1:65.

fluorescence as function of the PLR has reached a steady value (Fig. 1) and since the CD spectra of preparations with PLR 1:555 and 1:2222 in Fig. 6 are quite similar. The CD difference spectrum in Fig. 7 shows changes in LHCII conformation and microenvironment that could be associated with the transition from a weak protein- to a high protein-coupling regime. These changes likely include LHCII quencher sites, which are proposed to involve the pigments Chl*a*610, *a*611, *a*612 and Lut1 [2,13,16]. In the CD Q_y region, the bands at (+)662 nm and (−)673 nm are dominated by *a*611-*a*612 interactions [33]. The CD difference spectrum in Fig. 6 suggests that the *a*611-*a*612 excitonic interactions are enhanced at the high PLR. The extensive CD study of Akhtar et al. on LHCII in liposomes and detergent micelles concluded that CD changes at (−)437 and (+)484 are specific to LHCII-LHCII interactions [36]. Similar features are visible in the difference CD spectrum in Fig. 7. A negative band at 437 nm is also prominent in the difference spectrum comparing nanodiscs and proteoliposomes with low PLR (Fig. 4), but here the band in the *nanodisc* spectrum is more pronounced. This observation can be explained if we take LHCII-MSP protein-protein contacts in consideration. The CD band could represent a structural signature of LHCII-protein interactions, where the interaction partners are the neighboring LHCII

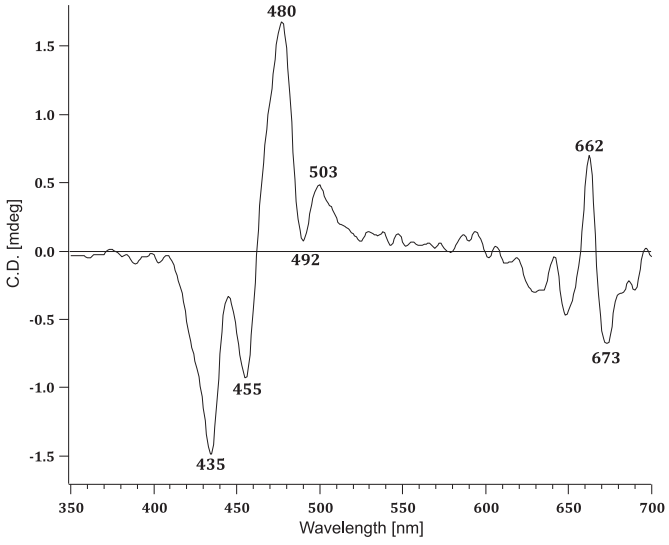

Fig. 7. CD difference spectrum of LHCII MGDG/DGDG/SQDG/PG proteoliposomes with PLR (1:65) – PLR (1:555).

complexes in crowded membranes or the MSP scaffold proteins in nanodiscs. The signature does not correlate with fluorescence quenching, since LHCII in nanodiscs retains its fully fluorescent state. The Soret region contains additional bands at (−)455 nm and at (−)492 and (+)503 nm, of which the latter two signatures have tentatively been attributed to changes in the configuration or micro-environment of Lut1 [8] and were observed for gel-immobilized LHCII trimer complexes, in which quenching was induced without protein aggregation, upon detergent removal. Increased Chl *a*612-Lut1 excitonic interactions are predicted to give a negative contribution to the CD signal at 492 nm [33]. On the other hand, the (−)492 nm band has been attributed to changes in the neoxanthin (Neo) xanthophyll that protrudes from the LHCII complexes [36] and the formation of LHCII aggregates *in vitro* and *in vivo* is associated with distortion of the Neo polyene chain [13]. Neo-Chl *b*608 interactions are also predicted to give a negative contribution to the CD signal at 492 nm. Our LHCII preparations also contain violaxanthin (Vio) that predominantly occupies the V1 site of LHCII where it is loosely bound. We cannot explude that some Vio was lost in the membrane reconstitution procedure, affecting the C.D. spectra. However, this will not influence the comparison between proteoliposomes with high and low protein densities.

Summarizing, the transition from a mild to strong fluorescence-quenched state, reminiscent of the transition from a light-harvesting to a photo protective state *in vivo*, is associated with CD changes involving enhanced *a*611-*a*612 interactions, and involving enhancedLut1-*a*612 interactions and/or alterations in the direct Neo environment. These pigments correspond well with LHCII quencher sites or with quenching-associated structural changes that have been proposed based on results from optical, Raman and NMR spectroscopy, and that were predicted by structure-based modeling studies [13,15,16,37,38]. Our results strongly suggest that the aggregation-induced LHCII fluorescence quenching at very low protein densities as observed in Fig. 1 is a different process that does not involve these typical C.D. features and does not reduce the fluorescence more than ~50%. This observation is in agreement with the observation in Holleboom et al. that suggest that, in addition to a carotenoid (Car)-Chl coupling-dependent quenching mechanism acting at high protein densities, another Car-Chl independent quenching mechanism is involved in a "weak-coupling" regime where the Chl-to-lipid molar ratio exceeds 1: 8 [11]. In the earlier study by Moya et al. aggregation-induced fluorescence quenching was studied in proteoliposomes with much higher protein densities than in our study, showing that average LHCII fluorescence lifetimes were reduced from 1.7 to 0.9 ns, compared to an average lifetime of 3.6 ns of LHCII in detergent solution [29]. We presume that these results report the protein-to-lipid regime where the transition from a mild to strong fluorescence-quenched state occurs, and not the transition occurring at the onset of aggregation that we followed in Fig. 1. Indeed, the most diluted proteoliposome preparations in the study of Moya et al. have a fluorescence yield that is already ~50% reduced compared to LHCII in detergent solution.

3.4. Orientation of LHCII insertion in preformed liposomes

Finally, we tested if with our liposome reconstitution method that follows the method of Rigaud [39], the LHCII complexes would insert in membranes with a preferential orientation. LHCII proteoliposomes with low protein to lipid ratios and LHCII in β-DM as a control were exposed to trypsin or chymotrypsin cleavage. Trypsin is known to cleave part of the N-terminal site of LHCII, while for well-folded LHCII complexes the C-terminal cleavage sites are shielded from cleavage and buried in the hydrophobic membrane phase. Random orientation of LHCII in liposomes should lead to 50% cleavage if half the LHCII have their N-terminal sites oriented inward in the liposome interiors. In contrast, the interactions of trypsin with LHCII in β-DM micelles should lead to 100% cleavage since all LHCII N-terminal sites are accessible. The cleavage experiments were repeated under different trypsin

incubation conditions, varying the temperature and incubation times. Fig. 8 shows a typical SDS-page analysis of a cleavage experiment. Strikingly, for LHCII proteoliposomes only a cleaved product band is observed, suggesting that all proteins are cleaved. For LHCII in β-DM micelles two cleavage products are found, which indicates that the protein is more exposed in detergent micelles. The two trypsin cleavage products are identified as 25 kD and 23.5 kD fragments of N-terminal-cleaved LHCII [40]. The results suggest a strong preferential orientation of LHCII in membranes, with its C-terminal site inserted and its N-terminal site exposed to the liposome exterior. No cleavage products were detected from chymotrypsin, that cleaves two aromatic-type amino acids (tryptophan and phenyl-alanine), instead of the polar residues (lysine and arginine) that are cleaved by trypsin (see SI Figs. S6 and S7 for possible cleavage sites). The absence of chymotrypsin cleavage products indicates that the aromatic residues are buried in the hydrophobic phase of the membrane or detergent micelle. The absence of smaller cleavage products confirms that all the LHCII complexes were incorporated in the proteoliposomes and were well-folded, trimeric complexes.

In native thylakoid membranes and in *in-vitro* membrane refolding studies, LHCII apo proteins insert in the membrane starting from their C-terminal site that is exposed to the lumen interior [40,41]. To the best of our knowledge, we are the first to observe preferential insertion of folded, native LHCII pigment-protein complexes upon membrane reconstitution. Preferential insertion of membrane proteins from mixed protein-detergent micelles into liposome membranes, as well as membrane insertion of membrane α-helices during folding and assembly *in vivo*, is driven by hydrophobicity of the protein terminal sites [42,43]. LHCII pigment-protein complexes contain several polar groups at both protein sites, but while at the C-terminal site positively- and negatively-charged residues are in close distance and may neutralize the net charges, the N-terminal site contains a distinct pattern of positive and negative patches [44]. Such pattern could prevent insertion via the N-terminal site. Trypsin cleavage experiments unfortunately only detect interactions at the LHCII N-terminal site. Adding a C-terminal tag by using recombinant LHCII could help to further clarify the direction of LHCII insertion using our reconstitution method.

Directional insertion requires a careful reconstitution protocol in which preformed liposomes are not solubilized during the protein insertion process. These conditions are maintained at low PLRs, where the onset of fluorescence quenching is observed. The low onset for aggregation-induced LHCII quenching in our experiments is indicative of strong attractive forces between the LHCII proteins. In native membranes, formation of membrane domains and the presence of MGDG could further promote aggregation by controlling membrane curvature.

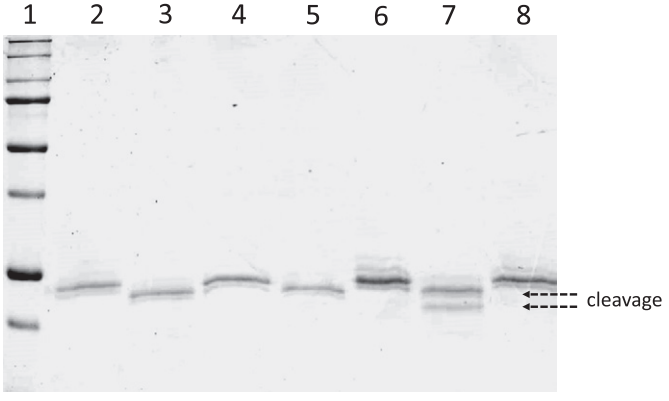

Fig. 8. SDS-page analysis of enzymatic cleavage experiments. From left to right: 1, marker; 2, LHCII proteoliposomes; 3, LHCII proteoliposomes + trypsin; 4, LHCII proteoliposomes + chymotrypsin; 5, LHCII proteoliposomes with trypsin and chymotrypsin; 6, LHCII in β-DM; 7, LHCII in β-DM + trypsin; 8, LHCIIin β-DM + chymotrypsin. Arrows indicate the height of cleavage product bands.

The low onset for quenching implies that studies using diluted LHCII proteoliposomes should take into account the vesicle dimensions in addition to the PLR, because quenched states are already produced when more than one LHCII protein *per vesicle* is present. For larger liposomes, these occasions will occur at lower PLRs. Strong attractive forces in LHCII *in-vitro* aggregates are often attributed to head-tail interactions, in which the proteins make non-native interfacial protein contacts. Our results however strongly suggest that also under experimental conditions where membrane-embedded LHCII complexes are uniformly oriented, as is the case *in vivo*, attractive protein interactions occur.

The data on LHCII lipid nanodiscs and highly diluted proteoliposomes demonstrate that excitation quenching in LHCII membranes is not induced by protein-lipid molecular interactions, but is controlled by the effects of aggregation. At low protein densities, attractive forces between the LHCII complexes cause mild quenching. At very high protein densities, the effect of lateral pressure caused by membrane crowding might produce the conformational changes into states where excitations are rapidly dissipated for efficient photo protection. While simple LHCII-lipid model systems have many limitations in mimicking native thylakoid membranes, it is interesting to note that they can reproduce the connectivity of active light-harvesting as well as the strong excitation quenching of photo protective states [21,29,45]. This notion suggests that lipid physico-chemical parameters and the molecular design of LHC complexes are sufficient elements to govern a flexible light-harvesting antenna.

4. Conclusions

We demonstrate that LHCII fluorescence quenching is not the result from a specific thylakoid lipid microenvironment, but is driven by LHCII protein-protein interactions. Diluting the protein to lipid ratios in LHCII proteoliposomes to a few proteins per liposome vesicle increases the fluorescence to reach the maximal Chl fluorescence, observed for LHCII in detergent micelles or in lipid nanodiscs. Increasing the PLR rapidly decreased the fluorescence yields to stabilize at a ~50% reduced yield at a PLR of 0.001, indicating (1) that strong LHCII-LHCII attractive interactions occur and (2) that this mild quenching process, occurring on the onset of aggregation, reaches equilibrium at protein densities of tens of LHCII trimers per vesicle. The CD results suggest that LHCII trimers in lipid nanodiscs are in contact with the MSP proteins, defining a size limit for protein incorporation into MSPE3D1 nanodiscs. The quenching process at the onset of aggregation is distinct from transition occurring at much higher protein densities. A comparison of LHCII proteoliposomes with low and very high protein densities allowed to us to detect the excitonic CD changes correlating with a second transition from mild to strongly quenched states. The CD changes in the infrared region are attributed to Chl*a*611–612 enhanced interactions, while alterations in the Soret band could originate from Chl-Lut1 or Chl-Neo enhanced interactions. These conformational changes correlate well with the quencher sites that have been proposed for the LHCII photo protective switch.

Transparency document

The Transparency document associated with this article can be found, in online version.

Acknowledgements

This work was supported by a VIDI grant (project number 723.012.103) of the Chemical Sciences division, Netherlands Organization of Scientific Research awarded to A. Pandit. M. C. A. Stuart, Electron Microscopy, Groningen Biomolecular Sciences and Biotechnology, Univ. of Groningen is kindly acknowledged for performing the cryo-electron microscopy experiments.

Appendix A. Supplementary data

Supplementary data to this article can be found online at http://dx.doi.org/10.1016/j.bbamem.2016.10.010.

References

[1] A.V. Ruban, M.P. Johnson, C.D. Duffy, The photoprotective molecular switch in the photosystem II antenna, Biochim. Biophys. Acta 1817 (1) (2012) 167–181.
[2] T.P. Kruger, et al., Controlled disorder in plant light-harvesting complex II explains its photoprotective role, Biophys. J. 102 (11) (2012) 2669–2676.
[3] S. Bode, et al., On the regulation of photosynthesis by excitonic interactions between carotenoids and chlorophylls, Proc. Natl. Acad. Sci. U. S. A. 106 (30) (2009) 12311–12316.
[4] A. Pandit, et al., Nuclear magnetic resonance secondary shifts of a light-harvesting 2 complex reveal local backbone perturbations induced by its higher-order interactions, Biochemistry 49 (3) (2010) 478–486.
[5] J. Cruz, et al., Plasticity in light reactions of photosynthesis for energy production and photoprotection, J. Exp. Bot. 56 (411) (2005) 395–406.
[6] L. Tian, E. Dinc, R. Croce, LHCII populations in different quenching states are present in the thylakoid membranes in a ratio that depends on the light conditions, J. Phys. Chem. Lett. 6 (12) (2015) 2339–2344.
[7] K. Petrou, E. Belgio, A.V. Ruban, pH sensitivity of chlorophyll fluorescence quenching is determined by the detergent/protein ratio and the state of LHCII aggregation, Biochim. Biophys. Acta BBA Bioenerg. 1837 (9) (2014) 1533–1539.
[8] C. Ilioaia, et al., Induction of efficient energy dissipation in the isolated light-harvesting complex of photosystem II in the absence of protein aggregation, J. Biol. Chem. 283 (43) (2008) 29505–29512.
[9] H. Kirchhoff, Structural changes of the thylakoid membrane network induced by high light stress in plant chloroplasts, Philos. Trans. R. Soc. London B Biol. Sci. 369 (1640) (2014).
[10] S. Haferkamp, et al., Efficient light harvesting by photosystem II requires an optimized protein packing density in grana thylakoids, J. Biol. Chem. 285 (22) (2010) 17020–17028.
[11] C.-P. Holleboom, et al., Carotenoid–chlorophyll coupling and fluorescence quenching correlate with protein packing density in grana-thylakoids, J. Phys. Chem. B 117 (38) (2013) 11022–11030.
[12] N.E. Holt, et al., Carotenoid cation formation and the regulation of photosynthetic light harvesting, Science 307 (5708) (2005) 433–436.
[13] A.V. Ruban, et al., Identification of a mechanism of photoprotective energy dissipation in higher plants, Nature 450 (7169) (2007) 575–578.
[14] Y. Miloslavina, et al., Far-red fluorescence: a direct spectroscopic marker for LHCII oligomer formation in non-photochemical quenching, FEBS Lett. 582 (25–26) (2008) 3625–3631.
[15] A. Pandit, et al., An NMR comparison of the light-harvesting complex II (LHCII) in active and photoprotective states reveals subtle changes in the chlorophyll a ground-state electronic structures, Biochim. Biophys. Acta Bioenerg. 1827 (6) (2013) 738–744.
[16] C.D.P. Duffy, A. Pandit, A. Ruban, Modeling the NMR signatures associated with the functional conformational switch in the major light-harvesting antenna of photosystem II in higher plants, Phys. Chem. Chem. Phys. 16 (12) (2014) 5571–5580.
[17] C. Ilioaia, et al., Photoprotection in plants involves a change in lutein 1 binding domain in the major light-harvesting complex of photosystem II, J. Biol. Chem. 286 (31) (2011) 27247–27254.
[18] J. Chmeliov, et al., The nature of self-regulation in photosynthetic light-harvesting antenna, Nat. Plants 2 (2016) 16045.
[19] J. Chmeliov, et al., Light harvesting in a fluctuating antenna, J. Am. Chem. Soc. 136 (25) (2014) 8963–8972.
[20] S. Schaller, et al., Regulation of LHCII aggregation by different thylakoid membrane lipids, Biochim. Biophys. Acta BBA Bioenerg. 1807 (3) (2011) 326–335.
[21] F. Zhou, et al., Effect of monogalactosyldiacylglycerol on the interaction between photosystem II core complex and its antenna complexes in liposomes of thylakoid lipids, Photosynth. Res. 99 (3) (2009) 185–193.
[22] L. Wilk, et al., Direct interaction of the major light-harvesting complex II and PsbS in nonphotochemical quenching, Proc. Natl. Acad. Sci. U. S. A. 110 (14) (2013) 5452–5456.
[23] A. Pandit, et al., Assembly of the major light-harvesting complex II in lipid nanodiscs, Biophys. J. 101 (10) (2011) 2507–2515.
[24] J.M. Graham, J.R. Harris, D. Rickwood, In Vitro Techniques Cell Biology Protocols, 2006 201–378.
[25] P.J.G. Butler, W. Kühlbrandt, Determination of the aggregate size in detergent solution of the light-harvesting chlorophyll a/b-protein complex from chloroplast membranes, Proc. Natl. Acad. Sci. 85 (11) (1988) 3797–3801.
[26] T.H. Bayburt, S.G. Sligar, Membrane protein assembly into nanodiscs, FEBS Lett. 584 (9) (2010) 1721–1727.
[27] M.S. Webb, B.R. Green, Biochemical and biophysical properties of thylakoid acyl lipids, Biochim. Biophys. Acta BBA Bioenerg. 1060 (2) (1991) 133–158.
[28] J. Jouhet, Importance of the hexagonal lipid phase in biological membrane organization, Front. Plant Sci. 4 (2013) 494.
[29] I. Moya, et al., Time-resolved fluorescence analysis of the photosystem II antenna proteins in detergent micelles and liposomes, Biochemistry 40 (42) (2001) 12552–12561.
[30] E. Belgio, et al., Higher plant photosystem II light-harvesting antenna, not the reaction center, determines the excited-state lifetime—both the maximum and the nonphotochemically quenched, Biophys. J. 102 (12) (2012) 2761–2771.
[31] S.E. Mansoor, K. Palczewski, D.L. Farrens, Rhodopsin self-associates in asolectin liposomes, Proc. Natl. Acad. Sci. U. S. A. 103 (9) (2006) 3060–3065.
[32] P.H. Lambrev, et al., Functional domain size in aggregates of light-harvesting complex II and thylakoid membranes, Biochim. Biophys. Acta BBA Bioenerg. 1807 (9) (2011) 1022–1031.
[33] S. Georgakopoulou, et al., Understanding the changes in the circular dichroism of light harvesting complex II upon varying its pigment composition and organization, Biochemistry 46 (16) (2007) 4745–4754.
[34] C. Yang, et al., Thermal stability of trimeric light-harvesting chlorophyll a/b complex (LHCIIb) in liposomes of thylakoid lipids, Biochim. Biophys. Acta BBA Bioenerg. 1757 (12) (2006) 1642–1648.
[35] Z. Liu, et al., Crystal structure of spinach major light-harvesting complex at 2.72 Å resolution, Nature 428 (6980) (2004) 287–292.
[36] P. Akhtar, et al., Pigment interactions in light-harvesting complex II in different molecular environments, J. Biol. Chem. 290 (8) (2015) 4877–4886.
[37] J. Chmeliov, et al., An 'all pigment' model of excitation quenching in LHCII, Phys. Chem. Chem. Phys. 17 (24) (2015) 15857–15867.
[38] A. Pandit, et al., An NMR comparison of the light-harvesting complex II (LHCII) in active and photoprotective states reveals subtle changes in the chlorophyll a ground-state electronic structures, Biochim. Biophys. Acta 1827 (6) (2013) 738–744.
[39] J.-L. Rigaud, D. Lévy, Reconstitution of Membrane Proteins into Liposomes, in Methods in Enzymology, Academic Press, 2003 65–86.
[40] T. Zapf, et al., Synthesis and functional reconstitution of light-harvesting complex II into polymeric membrane architectures, Angew. Chem. Int. Ed. 54 (49) (2015) 14664–14668.
[41] A. Kuttkat, R. Grimm, H. Paulsen, Light-harvesting chlorophyll a/b-binding protein inserted into isolated thylakoids binds pigments and is assembled into trimeric light- harvesting complex, Plant Physiol. 109 (4) (1995) 1267–1276.
[42] J.-L. Rigaud, B. Pitard, D. Levy, Reconstitution of membrane proteins into liposomes: application to energy-transducing membrane proteins. Biochimica et biophysica acta, Bioenergetics 1231 (3) (1995) 223–246.
[43] D.M. Engelman, T.A. Steitz, The spontaneous insertion of proteins into and across membranes: the helical hairpin hypothesis, Cell 23 (2) (1981) 411–422.
[44] R. Standfuss, et al., Mechanisms of photoprotection and nonphotochemical quenching in pea light-harvesting complex at 2.5 Å resolution, EMBO J. 24 (5) (2005) 919–928.
[45] R. Sun, et al., Direct energy transfer from the major antenna to the photosystem II core complexes in the absence of minor antennae in liposomes, Biochim. Biophys. Acta BBA Bioenerg. 1847 (2) (2015) 248–261.